International Journal of Luminescence and Applications (ISSN: 2277-6362)
Vol. 7, No. 3-4, October - December 2017. Article ID: 242. pp.417-422.

Synthesis, Photoluminescence, Charecterization of MgO Nanophosphors Influenced by Dy^{3+} Ions Concentrations

Gitanjali Sahu* and **Anubha S. Gour**

SOS in Physics and Astrophysics,
Pt. Ravishankar Shukla University, Raipur, Chhattisgarh, India.

Abstract— *The present paper reports the synthesis, characterization and photoluminescence (PL) studies of MgO:Dy^{3+} nanoparticles. In this work, MgO:Dy^{3+} nanophosphors were prepared through solution combustion synthesis method using magnesium nitrate as oxidizer and urea as a fuel. The as-obtained MgO:Dy^{3+} nanomaterials were characterized by powder X-ray diffraction (XRD), energy-dispersive X-ray (EDX) analysis, Fourier transformation infrared (FTIR) spectroscopy, scanning electron microscopy (SEM), high resolution transmission electron microscope (HRTEM), photoluminescence (PL) spectra and afterglow curve analysis. The cubic structure of the MgO phosphors is confirmed by XRD analysis and crystalline size calculated by Scherer's formula using XRD data shows the nanocrystalline nature of the phosphor. No phase change is observed with increasing concentrations of Dy^{3+} ions. The surface morphology of the prepared phosphors is determined by SEM, which shows a sphere-like structure and good connectivity of the grains. The confirmation of the nanocrystalline phosphors is examined by HRTEM analysis. The photoluminescence studies revealed that the emission spectra of the prepared phosphors shows the broad emission centered at 435 nm and 480 nm due to the transition arises from the 4f→5d defect band transition of Dy^{3+} ions. The afterglow decay characteristics of different as synthesized MgO:Dy^{3+} nanophosphors are conceptually described. This is the first reported that on the synthesis of nanocrystalline MgO:Dy^{3+} materials by combustion method using urea as a fuel.*

Keywords— *PL, XRD, EDX, SEM, HRTEM*

1. INTRODUCTION

II-VI semiconductor nanocrystals are recently developed class of nanomaterials whose unique photophysical properties are helping to create a new generation in the field of photonics and microelectronics. Owing to small size, nanoparticles show properties, which are surprisingly different from those of the bulk material. Since their properties can be engineered during synthesis and processing steps, the metal oxide nanomaterials are of great technological importance due to their grain size dependant properties. There are a number of methods for preparing nano-crystalline materials viz. Inert gas condensation, physical vapor deposition, laser ablation, chemical vapor deposition, sputtering, molecular beam epitaxy etc [1-6]. In addition there are a number of solution-chemistry routes also. Among the available solution-chemistry routes, the combustion technique is capable of producing the nanocrystalline powders of metal oxides at a lower calcinations temperature in a surprisingly short time. Generally the powder obtained by this technique has the highest degree of phase purity coupled with the improved powder characteristics like narrow particle size and better sinter ability [7-8]. The very high amount of heat generated during combustion manifests in the form of either flame or fire and hence, the process is termed as auto-combustion process. MgO is an exceptionally important material for its wide applications in catalysis, refractory materials, paints, superconductor products and so on. Recently, much research has been focused on the fabrication and characterization of MgO nanostructures due to novel properties superior to their bulk counterparts, as well as promising utilizations in optics, electronics and microelectronics. A lot of work has been done to research on the synthesis of this compound and many crystal morphologies are reported [9-15]. Recently the observations on the optical absorption studies of nano size MgO powder indicate that the synthesized MgO is quite suitable for adsorption and dissociation of polar molecules, toxic waste remediation, etc. Further it is also noted that the synthesized MgO nano powder contains F- and M-defect centres, which are responsible for creating energy levels within the band gap (7.8 eV) of MgO [16-18]. K.im et al. studied the effect of acetic acid addition to Magnesium methoxide on the stability of the precursor and the crystallization behaviour of sol-gel derived MgO nanosize powder [19]. Additionally, Chowdery and Kumar have synthesized MgO with high degree of crystallinity and tubular morphology using magnesium acetate as a precursor [20]. The aim of this work is to prepare MgO and cadmium doped MgO nanocrystals with different molar concentrations, study the effect of these dopants on the structural characteristics of MgO and correlate between the obtained structure characteristics and dielectric properties of the cadmium doped MgO nanocrystals. In

* *Corresponding Author: geet.rjn29@gmail.com*

the present study, the synthesis and micro structural characterization of MgO and Cd doped MgO nanoparticles synthesized by combustion method are discussed. Magnesium nitrate is used as an oxidizer and glycine as fuel. The studies were carried out for two fuel-to-oxidizer ratios (ψ = 1:0.9). The variations of lattice parameters, crystalline size and band gap were studied. Band gaps of MgO and Cd doped MgO were determined by UV-vis absorption edge [21-22]. Important synthesis parameters were also probed for their effects on the nanocrystalline optical properties via photoluminescence measurements, and dielectric studies.

Kaviyarasu et al. [23] have studied the Synthesis and characterization studies of cadmium doped MgO nanocrystals for optoelectronics application. He examined the progress in adapting these nanomaterials for several predominantly photonics device fabrication by autocombustion method followed by characterization studies. Magnesium oxide (MgO) and Cd doped Magnesium oxide nanoparticles were characterized by X-ray powder diffraction and the peaks are quite agreeable with the pure phase cubic structure. The XRD pattern confirms the crystallinity and phase purity of the pure and doped samples. UV-vis-NIR study of the samples indicated a blue shift in the band gap for both the pure and doped ones. Photoluminescence measurements reveal the systematic shift of the emission band towards the lower wavelength thereby ascertaining the quantum confinement effect. Photoluminescence spectra of pure MgO and Cd doped MgO were investigated, showing emission peaks around 475 nm relating to new energy levels induced by defects or defect levels generation. The SEM results reveal that the resultant nanopowders are porous and agglomerated with polycrystalline nano entities. Field emission scanning electron microscopic studies showed that the average size of the nanoparticles were 20 nm and 33 nm respectively. The dielectric loss of the pure and Cd doped MgO samples decreases with increase in frequency. Similar trend is observed for the dielectric constant also.

Balamurugan et al. [24] have studied that the nanocrystalline MgO particles was prepared through combustion method using magnesium nitrate as oxidizer and hexamine as a fuel. The materials obtained by combustion method were subsequently annealed at 800 ^{0}C for 3 h to improve the crystallinity and phase purity.The obtained MgO nanomaterials were characterized by powder X-ray diffraction analysis (XRD), infrared (IR) spectroscopy, photoluminescence (PL), near-infrared (NIR) spectroscopy, and scanning electron microscopy (SEM). The cubic crystal structure with lattice parameter, a = 0.4210(4)nm with average crystalline size of 22 nm, is obtained for the nano- MgO particles.The PL emission spectrumof nanocrystalline MgOmaterials exhibits three emission peaks at 432, 465, and 495nm which are due to various structural defects. The SEM results expose the fact that the MgO nanomaterials are seemingly porous and highly agglomerated with fine particles. Owing to the higher reflectance of prepared nanocrystalline MgO, it can be used as NIR reflective pigments. The present results prove that the combustion technique using hexamine can produce the materials with high crystallinity. To the best of our knowledge, this is the first report on the synthesis of nanocrystalline MgO materials by combustion method using hexamine as a fuel.

The present paper reports the synthesis, characterization and photoluminescence studies of MgO:Dy^{3+} nanoparticles prepared by solution combustion synthesis method using urea as a fuel., and discusses the salient features of PL in detail.

1.1 Experimental

The starting raw materials are magnesium nitrate [$Mg(NO_3)_2.6H_2O$] urea [NH^2CONH^2] and dysprosium nitrate. These raw materials were firstly weighted first and were taken in mortar pistal and mixed it properly for one hour. After mixing, these materials are placed in crucible was then introduced into muffle furnace at 550°C for 20 min as the ignition occurs the reaction occurs vigorously for few seconds and the fluffy substance was obtained. Based on mass ratio of the experiment the overall reaction equation could be expressed as follows:

$$6[Mg(NO_3)_2.6H_2O]+6[Dy(NO_3)_3.6H_2O]+28[NH_2CONH_2] = 6MgO:Dy+43N_2+28CO_2$$

The morphologies and sizes of the MgO:Dy^{3+} nanoparticles were determined by X-ray diffraction (XRD) studies with Cu Kα radiation (λ=1.5418Å). XRD data were collected over the range 20-70^0 at room temperature. X-ray diffraction patterns were obtained using a Rigaku Rotating Anode (H-3R) diffractometer. In XRD the particle size was calculated using the Debye-Scherrer formula. The particle size was also calculated using the scanning electron microscope (SEM) and high resolution transmission electron microscope (HRTEM) methods. The photoluminescence were recorded with the help of a Shimadzu spectroflurophotometer RF 5301PC.

2. RESULT AND DISSCUSSION

2.1 Structural Analysis

2.1.1 X-Ray Diffraction (XRD) Study

The XRD patterns for the samples are shown in Fig. 1 MgO:Dy^{3+} nanocrystals for four different concentrations (0.2, 0.4, 0.6 and 0.8 mol%) of Dysprosium, three different peaks are obtained at 2θ. This shows that the samples have cubic structure and the peaks correspond to diffraction at (111), (200) and (220) planes, respectively. The size of the particle has been computed from the width of the first peak using Debye-Scherrer formula [25] given below:

$$D=\frac{K\lambda}{\beta cos\theta} \quad (1)$$

where K is constant (K=0.9), λ the wavelength of X-ray, β the full width at half maximum and θ is Bragg angle. The particle sizes obtained from XRD were in the range 28-43 nm. The Debye-Scherrer equation has a few limitations. Table 1. Shows that the Structural parameters of MgO nanocrystalline with different concentration of Dy^{3+}. Moreover, the presence of defects in a significant amount causes an additional enlargement of the diffraction line. These problems can be overcome by measuring the particle size by SEM and HRTEM.

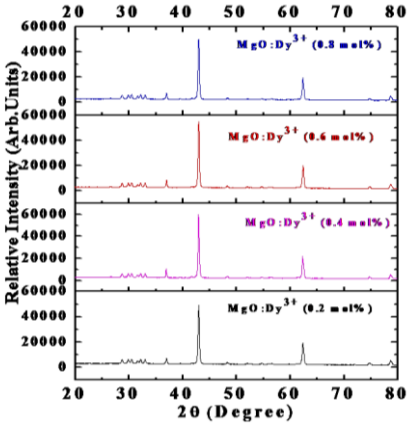

Fig. 1. X-ray patterns of MgO nanocrystalline with different concentration of Dy^{3+}

Table 1: Structural parameters of MgO nanocrystalline with different concentration of Dy^{3+}

2θ (Degree)	*FWHM(β) (Radian)*	*hkl*	*Crystalline Size (D) (nm)*
(a) MgO:Dy^{3+} (0.2 mol%)			
36.95	0.00576	111	29
42.97	0.00360	200	42
62.34	0.00576	220	35
(b) MgO:Dy^{3+} (0.4 mol%)			
36.85	0.00566	111	28
42.87	0.00350	200	41
62.45	0.00556	220	34
(c) MgO:Dy^{3+} (0.6 mol%)			
36.75	0.00596	111	28
42.77	0.00350	200	43
62.32	0.00556	220	36
(d) MgO:Dy^{3+} (0.8 mol%)			
36.55	0.00566	111	30
42.56	0.00360	200	43
62.40	0.00566	220	35

2.1.2 EDX (Energy Dispersive X-Ray)

Fig.2a shows the spectrum obtained by EDX samples and the sample spectrum 100% of Mg metal was observed in the sample corresponding to peak shown in the Fig.2b. In sample the inclusion of Dy^{3+} is shown in the corresponding peaks. From the data it is observed that the synthesized sample contains about Mg, O and Dy with 55.71%, 44.32% and 0.87% of atomic percentage respectively which agrees with expected value.

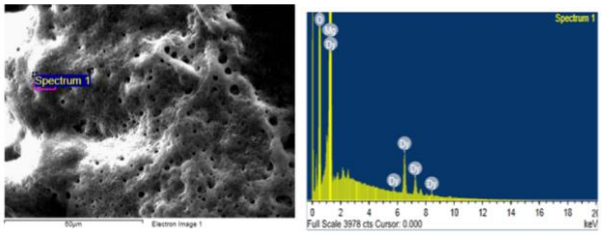

Fig. 2: (a,b) EDX spectra of MgO:Dy^{3+} nanocrysalline phosphors

2.1.3 Scanning Electron Microscope (SEM)

Figure 3(a,b,c,d) shows the SEM image of MgO:Dy^{3+} nanoparticles. The SEM image is carried out by using Zeiss. Evo 18 Special Edition in order to analyse the structure and morphology of doped samples. SEM was used for the morphological study of MgO Doped with Dy^{3+}. The instrument was accelerated at voltage of 10 Kv and the samples were scanned at a working distance of 8.5 mm. The SEM images for the MgO doped with dysprosium samples are shown in Fig.3(a,b,c,d).

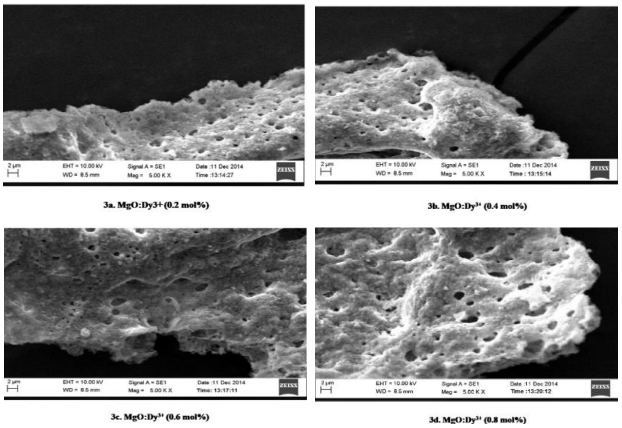

Fig. 3: (a,b,c,d) SEM images of different nanocrystalline MgO:Dy^{3+} phosphors.

2.1.4 High Resolution Transmission Electron Microscope (HRTEM)

A typical HRTEM image of MgO:Dy^{3+} nanoparticles is shown in Fig.4 and Fig.4a,b,c,d, respectively. The particle size obtained from HRTEM image is found to be in the range of 20 nm. Fig.5a,b,c,d, of HRTEM image clearly shows that the particles size is spherical. The lattice

fringes visible in the HRTEM micrograph are indicative of the crystalline nature of the particles. The three

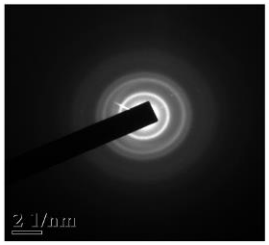

Fig. 4: The SAED pattern of MgO:Dy^{3+} nanocrystalline phosphors.

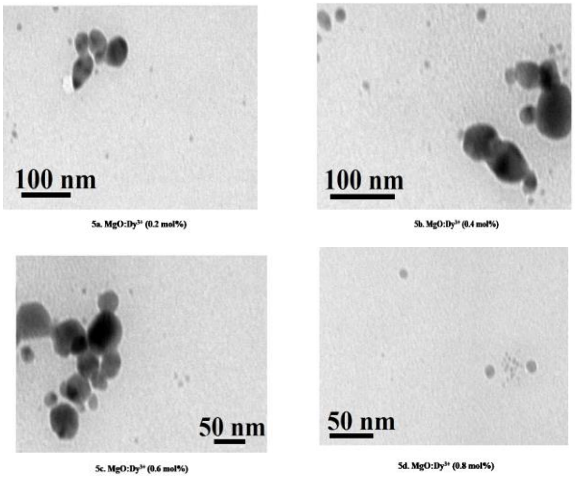

Fig. 5: (a,b,c,d) HRTEM images of different nanocrystalline of MgO:Dy^{3+} phosphors.

diffraction rings in the EDX patterns correspond to the (111), (200) and (220) reflections, confirming the cubic structure in accordance with XRD results.

2.1.5 Fourier Transforms Infrared Spectra (FTIR)

Figure 6 shows FTIR Spectra of MgO:Dy^{3+} particles are peaks at 3448 cm^{-1} and 2450 cm^{-1} corresponding to the O–H stretching mode of hydroxyl groups were present on the surface due to moisture. Peak at 1672 cm^{-1} was attributed to the bending vibration of water molecule. There are also small narrow bands at 1002 cm^{-1} which are due to the

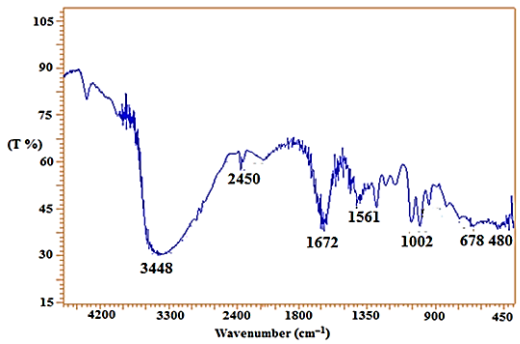

Fig. 6: FTIR Spectra of MgO:Dy^{3+} nanocrystalline phosphors.

oxygen stretching and bending frequency. In additions the bands at 1561 cm^{-1} and 1672 cm^{-1} are due to C-H stretching. The major peaks at 480 cm^{-1}, 678 cm^{-1} which confirmed the presence of Mg-O vibrations.

3.1 OPTICAL PROPERTIES

3.1.1 Photoluminescence Studies of MgO:Dy^{3+} Nanocrystalline

The excitation spectra are 220, 277, and 325 nm and emission spectra are 435, 480 nm, and 510 nm of the different MgO:Dy^{3+} nanophosphors are shown in Fig. 7(a) and Fig.7(b) respectively. The broad band excitation spectra of different MgO:Dy^{3+} nanophosphors exhibits a very strong absorption in the band between 435 and 480 nm, accompanied by avery weak band around 510 nm and an intense band at 435 and 480 nm attributed to the 4f→5d transitions of Dy^{3+} ions. Therefore, it is concluded that MgO:Dy^{3+} phosphors can be excited efficiently by UV as well as visible light. The emission spectra of synthesized MgO nanophosphors with variable concentrations of Dy^{3+} shows broad emission band extending in the UV-vis region from 400 to 550 nm, attributed to the electron transition from 5d lowest energy level of Dy^{3+} to the $^2F_{5/2}$ to $^2F_{7/2}$ manifolds split by spin orbits coupling [26]. The broadness of the emission peak is described to emission from more than one enrgy level. The emission peaks centered at 435 nm and 480 nm (blue region) and 510 nm (green region) are attributes to radiative recombination of photogenerated hole with electron occupying the surface defects. The energy levels of these defects centers exist in the forbidden energy gap of MgO nanophosphors. During the intial illumination, Dy^{3+} as the dopant ion allows more enrgy to be stored, prolonging (0.4 mol% of Dy^{3+} ion) the emission intensity of MgO nanophosphors. With further increases in the Dy^{3+} ion concentration (to 0.6 mol%), the intensity decreases. This quenching between two identical centers of two Dy^{3+} ions is explained by the resonant energy transfer model [26]. Figure 7(b) shows that the percentage variation in PL intensity with increasing Dy^{3+} dopant concentration.

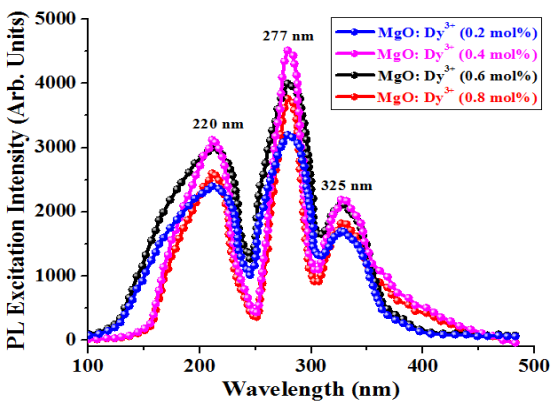

Fig. 7: (a) PL excitation spectra of different nanocrystalline MgO:Dy^{3+} phosphors

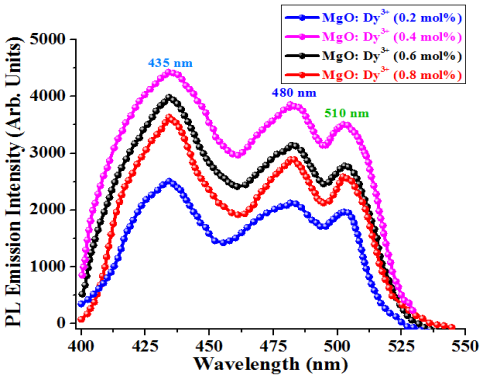

Fig. 7: (b) PL emission spectra of different nanocrystalline MgO:Dy^{3+} phosphors

4. AFTERGLOW DECAY CHARACTERISTICS

Following irradiation by UV light (λ = 220 nm, 275 nm and 325 nm) for 5 min at room temperature, the afterglow decay measurement was carried out for different MgO:Dy^{3+} (0.2, 0.4, 0.6 and 0.8 mol%) nanophosphors, as shown in Fig. 8(a). The presence of Dy^{3+} ions is responsible for the generation of appropriate traps needed for the afterglow decay behavior. The initial luminescence intensity and decay times are functions of the Dy^{3+} concentration, such that the nanophosphor with 0.4 mol% of Dy^{3+} has the highest initial intensity and longest decay time (110 ns); furthermore, the decay time decreased at concentrations beyond 0.6 mol% of Dy^{3+}. The decay curves are fitted using the first-order exponential decay function, as shown in Fig. 8(b):

$$I=A \exp\left(\frac{-t}{\tau}\right) \quad (2)$$

Where I is the intensity at any time t, A is a constant and τ is the rapid decay lifetime for the exponential component. The fitted decay parameters are listed in Table 3. The rapid decay lifetime may be attributed to the shallow trapping states requiring low energy to de-trap the trapped electrons from these states, accompanied by fast decay of the luminescence intensity.

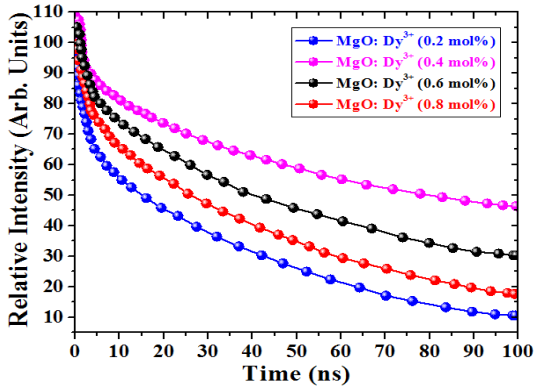

Fig. 8: (a) Afterglow decay curve of different nanocrystalline MgO:Dy3+ phosphors after exposure to UV light (λ=220, 277,315 nm) for 5 min

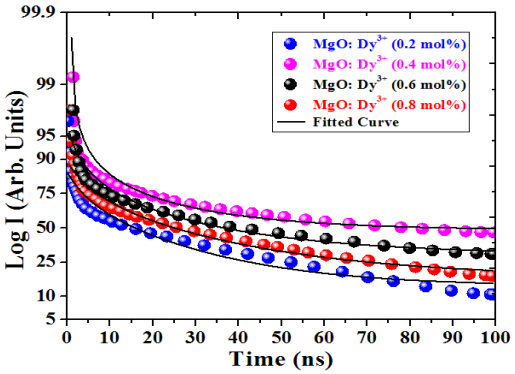

Fig. 8: (b) The first order exponentially fitted curves of different nanocrystalline MgO:Dy3+ phosphors using Origin Pro 8.5 software.

5. CONCLUSIONS

The MgO nanophosphors doped with varying concentrations of Dy^{3+} ions have been successfully synthesized by solid state combustion method. The structural characterization in terms of XRD, SEM, HRTEM, SAED and EDX validate the nano size of prepared samples. The average crystallite size for different MgO: Dy^{3+} was estimated to be 28-43 nm. The PL emission peaks at 435 and 480 nm (blue region) and 510 nm (green region) are assigned respectively to the $^2T_{2g}$ (5d)→$2F_{5/2}$ (^{4}f), $2F_{7/2}$ (4f) transitions of the Dy^{3+} ions. At 0.4 mol% concentration of Dy^{3+} ions, the PL intensity is found to be maximum and, further increase in Ce3+ concentration quenches the PL emission intensity due to resonant energy transfer. the relative PL intensity was very low due to creation of more and more defects which behaved like quenching centers as a result of decrease in crystallite size. The decay lifetime was found to be maximum (89 ns) for Dy^{3+} (0.4%) naophosphors respectively. The intense emission upon UV-light excitation suggests that MgO: Dy^{3+} nanophosphor can be used as a potential blue-emitting phosphor for optical devices such as white light LEDs, etc.

REFERENCES

[1] V Haubold, R. Bohn, R Birringer, Nanocrystalline intermetallic compounds--structure and mechanical properties, "Mater. Sci. Eng., A153(1992) 679-685.

[2] J.L.Vosen,W. Kern, Thin films precursors (Academic Press Boston) 1991.

[3] W.S. Hu, Z.G.Liu, D. Fency, Comparative study of laser ablation techniques for fabricating nanocrystalline SnO_2 thin films for sensors, Mater. Lett., 28(1996)369-372.

[4] W.Kern, R.S.Roster, J.Vac., Advance in the deposition processes for passivation film, Sci., Techno, 14(1977)1082-1085.

[5] T.C.Tisone, P.D.Cruzan, J. Vac., Low-voltage triode sputtering with a confined plasma: Part V—

Application to back-sputter definition, Sci. Technol, 12(1975) 677-680.

[6] A.Y.Cha, K.Y.Cheng, Growth of extremely uniform layers by rotating substrate holder with molecular beam epitaxy for applications to electro- optic and microwave devices, Appl. Phys. Lett.,38(1981) 360-366.

[7] S. B. Kondawar, M.J. Hedau, V. A. Tabhane, S. P. Dongare, U. B. Mahatme, R. A. Mondal, J. Mod., Studies on Chemically Synthesized Doped Poly(O-Anisidine) And Copoly{aniline-(o-anisidine)}, phys. lett. b, 20(2006)1461-1470.

[8] Y.He, Preparation of polyaniline/nano-ZnO composites via a novel Pickering emulsion route, Powder Technol., 147 (2004) 59-63.

[9] S.H.C. Liang, I.D. Gay, Synthesis and Characterization Studies of Mgo-Nio Nanocomposites, J. Catal., 101(1986) 293-295.

[10] P.D. Yang, C.M. Lieber, Nanorod superconductor composites of a pathway to materials with highcritical current density, Science, 273(1996)1836-1839.

[11] K. Hojrup Hansen, S. Ferrero, C. R. Henry, Nucleation and growth kinetics of gold nanoparticles on MgO (1 0 0) studied by UHV-AFM, Appl. Surf. Sci., 226(2004)247-250.

[12] Xiao feng Lu,Youhai Yu, Liang Chen, Huaping Mao, Wanjin Zhang & Yen Wei, Preparation and characterization of polyaniline microwires containing CdS nanoparticles,Chem. Commun., 1522(2004)1522-1523.

[13] V. Mishakov, A.F. Bedilo, R.M. Richards, V.V. Chesnokov, A.M. Volodin, V.I. Zaikovskii, R.A. Buyanov, K.J. Klabunde, Nanocrystalline MgO as a Dehydrohalogenation Catalyst, J. Catal., 206(2002) 40-43.

[14] X. Y. Ma, G. X. Lu, B. J. Yang, Study of the luminescence characteristics of cadmium sulfide quantum dots in a sulfonic group polyaniline (SPAn) film Applied Surface Science, 187(2002) 235-238.

[15] Y.Li, X. Zhang, X. Tao, J. Xu, F. Chen, W.Huang, F. Liu, Growth mechanism of multi-walled carbon nanotubes with or without bundles by catalytic deposition of methane on Mo/MgO, Chem. Phys. Lett,. 386(2004) 105-108.

[16] Fan Jun, Ji Xin, Zhang Weiguang, Yan Yunhui, CJI, 6(2004)45-49.

[17] Y.D. Li, M. Sui, Y. Ding, G.H. Zhang, J. Zhuang, C. Wang, Communication: The solution synthesis of Mg $(OH)_2$ nanorods is discussed with emphasis on the influence of experimental conditions on the morphology of the products. A templating mechanism is suggested, Adv. Mater., 12(2000)818- 820.

[18] M.S. Mel'gunov, V.B. Fenelonov, E.A. Mel'gunova, Textural Changes during Topochemical Decomposition of Nanocrystalline $Mg(OH)_2$ to MgO J. Phys. Chem, 107(2003) 2427-2430.

[19] Ashok Kumar, Jitendra Kumar, On the synthesis and optical absorption studies of nano-size magnesium oxide powder, J. of Physics and Chemistry of solids, 69(2008) 2764-2772.

[20] J.Y.Kim, H.S.Jung, K.S.Hong, "Effects of Acetic Acid on the Crystallization Temperature of Sol-Gel Derived MgO Nano-Powders and Thin Films, J. Am.cerm., 88(2005) 784-787.

[21] D. Y. Godowsky, A. E. Varfolomeev, D. F. Zaretsky, Preparation of nanocomposites of polyaniline and inorganic semiconductors, J. Mater. Chem, 11(2001)2465-2469.

[22] A.Chowdhury, J.Kumar, Structural, thermal, dielectric studies on sol–gel derived MgO from non-alkoxide route, Sci.technol., 22(2006)1249-1254.

[23] K. Kaviyarasu and Prem Anand Devarajan, Pelagia Research Library, Synthesis and characterization studies of cadmium doped MgO nanocrystals for optoelectronics application, Advances in Applied Science Research, 2 (2011) 131-138.

[24] S. Balamurugan, L. Ashna, and P. Parthiban1, Synthesis of Nanocrystalline MgO Particles by Combustion Fallowed by Annealing Method Using Hexamine as a Fuel, Hindawi Publishing Corporation Journal of Nanotechnology Volume 2014, Article ID 841803, 6 pages http://dx.doi.org/10.1155/2014/841803.

[25] S. Mahamuni, A. Khosravi, M. Kundu, A. Kshrisagar, A. Bedekar, DB.Avasare, Thiophenol capped ZnS quantum dots., J Appl Phys, 73 (1993) 5237.

[26] M. Emena, N. Külcüb and Ahmet N. Yazıci, Synthesis, characterization and luminescence properties of the long afterglow Phosphor $Ba_4Al_{14}O_{25}$:Eu,Dy, European Journal of Chemistry, 1 (1) (2010) 28-32.